Original Article
Yonsei Med J 2024 May;65(5):283-292
https://doi.org/10.3349/ymj.2023.0323
Yonsei Medical Journal
YMJ
pISSN: 0513-5796 · eISSN: 1976-2437

Diffusion- and Perfusion-Weighted MRI Radiomics for Survival Prediction in Patients with Lower-Grade Gliomas

Chae Jung Park[1], Sooyon Kim[2], Kyunghwa Han[3], Sung Soo Ahn[3], Dain Kim[4], Yae Won Park[3], Jong Hee Chang[5], Se Hoon Kim[6], and Seung-Koo Lee[3]

[1]Department of Radiology, Research Institute of Radiological Science, Yongin Severance Hospital, Yonsei University College of Medicine, Seoul;
[2]Department of Applied Statistics, Yonsei University, Seoul;
[3]Department of Radiology, Center for Clinical Imaging Data Science, Research Institute of Radiological Sciences, Severance Hospital, Yonsei University College of Medicine, Seoul;
[4]Graduate School of Artificial Intelligence, Pohang University of Science and Technology, Pohang;
[5]Department of Neurosurgery, Yonsei University College of Medicine, Seoul;
[6]Department of Pathology, Yonsei University College of Medicine, Seoul, Korea.

Purpose: Lower-grade gliomas of histologic grades 2 and 3 follow heterogenous clinical outcomes, which necessitates risk stratification. This study aimed to evaluate whether diffusion-weighted and perfusion-weighted MRI radiomics allow overall survival (OS) prediction in patients with lower-grade gliomas and investigate its prognostic value.

Materials and Methods: In this retrospective study, radiomic features were extracted from apparent diffusion coefficient, relative cerebral blood volume map, and Ktrans map in patients with pathologically confirmed lower-grade gliomas (January 2012–February 2019). The radiomics risk score (RRS) calculated from selected features constituted a radiomics model. Multivariable Cox regression analysis, including clinical features and RRS, was performed. The models' integrated area under the receiver operating characteristic curves (iAUCs) were compared. The radiomics model combined with clinical features was presented as a nomogram.

Results: The study included 129 patients (median age, 44 years; interquartile range, 37–57 years; 63 female): 90 patients for training set and 39 patients for test set. The RRS was an independent risk factor for OS with a hazard ratio of 6.01. The combined clinical and radiomics model achieved superior performance for OS prediction compared to the clinical model in both training (iAUC, 0.82 vs. 0.72, p=0.002) and test sets (0.88 vs. 0.76, p=0.04). The radiomics nomogram combined with clinical features exhibited good agreement between the actual and predicted OS with C-index of 0.83 and 0.87 in the training and test sets, respectively.

Conclusion: Adding diffusion- and perfusion-weighted MRI radiomics to clinical features improved survival prediction in lower-grade glioma.

Key Words: Glioma, isocitrate dehydrogenase, magnetic resonance imaging, prognosis, nomogram

Received: August 9, 2023 **Revised:** October 27, 2023
Accepted: December 13, 2023 **Published online:** March 14, 2024
Corresponding author: Sung Soo Ahn, MD, PhD, Department of Radiology, Center for Clinical Imaging Data Science, Research Institute of Radiological Sciences, Severance Hospital, Yonsei University College of Medicine, 50-1 Yonsei-ro, Seodaemun-gu, Seoul 03722, Korea.
E-mail: SUNGSOO@yuhs.ac

•The authors have no potential conflicts of interest to disclose.

INTRODUCTION

Lower-grade gliomas of the World Health Organization (WHO) CNS grades 2 and 3 are infiltrative neoplasms with variable clinical outcomes and widely ranging survival, from 1 to 15 years.[1] Isocitrate dehydrogenase (IDH) is one of the key genetic events leading to glioma stratification with significantly different survival rates in adult-type diffuse gliomas.[2,3] However, heterogenous clinical outcomes have been reported in lower-grade gliomas with or without IDH mutation, according to the variable combination of genetic profiles.[4,5] The surgery is a

mainstay of therapy for lower-grade gliomas; however, the precise management after surgical resection, such as radiation or chemotherapy, remains to be determined.[6] Adjuvant radiation and chemotherapy are selectively performed by weighing the risk-benefit ratio of treatment for each individual patient, and they are usually performed when a patient is deemed high-risk.[6] If the patient is considered as low-risk, aggressive postoperative treatment should be spared, as those treatments are often accompanied by adverse effects.[7] Therefore, it would be beneficial if MRI could stratify lower-grade glioma patients according to their risk and identify patients with worse prognosis, better addressing specific treatment needs.

Physiological biomarkers from diffusion-weighted imaging (DWI) and perfusion-weighted imaging (PWI) have been largely investigated in patients with gliomas. The DWI-derived apparent diffusion coefficient (ADC) reflects cellularity within the tumor. Dynamic susceptibility contrast (DSC) imaging allows for the measurement of cerebral blood volume (CBV), a surrogate marker for vascular proliferation and tumor angiogenesis, whereas dynamic contrast-enhanced (DCE) imaging allows the evaluation of the blood-brain barrier integrity by measuring quantitative permeability parameters.[8] Advanced MRI protocols involving DWI, DSC, or DCE can potentially discriminate grades and predict specific genetic mutations or prognosis in patients with gliomas.[9-11]

Radiomics exploits MRI data extracting high-dimensional quantitative imaging features, such as intensity distributions, spatial relationships, textural heterogeneity, and shape descriptors.[12] Since radiomics models use high-throughput imaging features, hidden information, which may be visually imperceptible, can be revealed.[13] Conventional MRI-derived radiomics has been adopted in patients with lower-grade gliomas to detect molecular subtypes including IDH mutation status, predict survival, or predict responses from chemotherapeutic agents.[14-17] Previous studies using DWI or PWI radiomics showed that these advanced MRI radiomics had good performance in determining the tumor grade or predicting specific genetic mutations in lower-grade gliomas.[18,19] However, to the best of our knowledge, the prognostic significance of DWI or PWI radiomics to predict survival in patients with lower-grade gliomas has not been well investigated.

We hypothesized that MRI radiomics derived from ADC and perfusion maps could improve the survival prediction of clinical profiles in patients with lower-grade gliomas. Therefore, this study aimed to evaluate whether radiomics allow risk stratification in preoperative settings in patients with lower-grade gliomas and to investigate the added prognostic value of DWI or PWI radiomics over clinical features alone.

MATERIALS AND METHODS

This retrospective study was approved by the Institutional Review Board of our hospital (No. 4-2021-1665), and the requirement to obtain informed patient consent was waived.

Patients

From January 2012 to February 2019, a total of 283 patients with pathologically confirmed lower-grade gliomas were identified. Patients with lower-grade gliomas who underwent preoperative MRI were included. Patients were excluded if they met any of the following criteria: 1) previous history of brain surgery or treatment (i.e., radiation therapy or chemotherapy, n=21); 2) age <18 years (n=16); 3) no preoperative MRI (n=12); 4) no DWI in the preoperative MRI (n=4); 5) either DSC or DCE not available in the preoperative MRI (n=99); or 6) error in preprocessing (n=2). Finally, 129 patients with lower-grade gliomas and preoperative MRI, including DWI, DSC, and DCE, were enrolled in this study (Fig. 1). Among them, 54 (41.9%) patients had WHO grade II gliomas and 75 (58.1%) patients had grade III gliomas.

Patients who had a pathologic diagnosis between 2015–2019

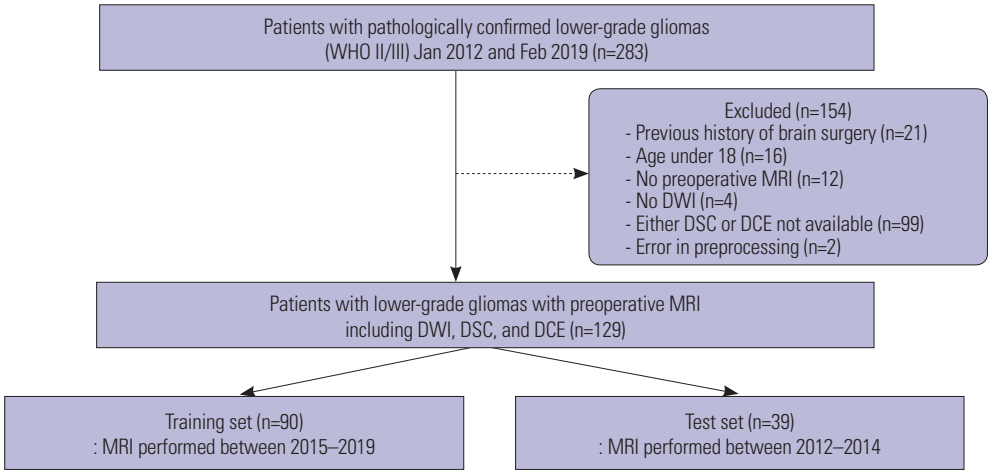

Fig. 1. Flowchart of the patient population. WHO, World Health Organization; DWI, diffusion-weighted imaging; DSC, dynamic susceptibility contrast; DCE, dynamic contrast-enhanced.

https://doi.org/10.3349/ymj.2023.0323

and 2012–2014 were allocated to the training and test sets, respectively.

The extent of tumor resection was determined by visually comparing the preoperative and postoperative lesion volume on both fluid-attenuated inversion recovery (FLAIR) and contrast-enhanced T1-weighted imaging (T1C), in conjunction with the surgeons' intraoperative impressions, classified into one of three categories: gross total, subtotal (<100% and ≥75% of gross tumor removal)/partial (<75% of gross tumor removal) resection, or biopsy only. The Karnofsky Performance Status (KPS) was determined preoperatively and retrieved from electronic medical records.

Overall survival (OS) was used as a clinical outcome, and it was defined as the number of days from the initial surgery (i.e., tumor resection or biopsy) to either patient death or the date of the last follow-up.

MR image acquisition and perfusion MRI preprocessing

The detailed MR image acquisition parameters and the preprocessing steps of DCE and DSC MRI are presented in Supplementary Material (only online). Among DCE MRI-related parameters, Ktrans, which denotes tissue permeability,[20] is the most widely investigated and useful imaging biomarker for glioma grading,[21,22] prediction of molecular status,[23] and prediction of prognosis.[24,25] Relative CBV (rCBV) also proved its significant correlation with tumor grade and prognosis in gliomas,[26] which is usually the only investigated parameter among DSC MRI parameters. Therefore, Ktrans map from DCE MRI and rCBV map from DSC MRI were used for further analysis.

Image pre-processing and radiomic feature extraction

FLAIR and ADC preprocessing was performed to standardize data analysis among patients. A 1-mm isovoxel resampling of the images was performed with bias field correction using the N4 bias field correction algorithm. Signal intensity normalization was performed by applying the z-score. Preprocessing of the rCBV map and Ktrans map only included 1-mm isovoxel resampling. Tumor segmentation was performed on FLAIR image by a neuroradiologist with 7 years of experience and confirmed by another senior neuroradiologist with 14 years of experience, who were both blinded to the clinical information. Both the infiltrative tumor and edema, which show high signal intensity on FLAIR, were segmented, including both enhancing and non-enhancing tumors. The segmentation was performed using semiautomatic method of signal intensity threshold, which was provided by the 3D slicer software (version 4.11.0).[27] Then, ADC images were co-registered to FLAIR images.

Radiomic features extracted from each mask were calculated automatically with an open-source Python-based module (PyRadiomics, version 2.0),[28] adherent to the Image Biomarker Standardization Initiative.[29] The features included the following: 1) 14 shape features; 2) 18 first-order features; and 3) 75 second-order features, including gray level co-occurrence matrix, gray level run-length matrix, gray level size zone matrix, gray level dependence matrix, and neighboring gray tone difference matrix. Overall, 107 radiomic features were extracted from each sequence. Among them, 14 shape features were identical along different sequences. Therefore, 293 features were extracted from ADC, rCBV and Ktrans maps. The pipelines for radiomics feature extraction are presented in Fig. 2.

Construction of the radiomics risk score

Due to the relatively large number of imaging variables compared with the number of events, the least absolute shrinkage and selection operator was used to select important features to minimize the potential risk for overfitting by shrinking the regression coefficients of irrelevant variables toward zero.[30] The performance of these methods was tested by 10-fold cross-validation with 100 replications to enhance the generalizability of the results. A radiomics risk score (RRS) was calculated for each patient using a linear combination of frequently selected features, weighted according to their regression coefficients. The RRSs calculated from the selected features from the ADC and from both CBV and Ktrans maps constituted a DWI radiomics and PWI radiomics model, respectively.

Model development based on multivariable Cox regression analysis

Univariable analysis of RRS and clinicopathologic features—age, sex, KPS, postoperative treatment (i.e., chemotherapy or radiation therapy), extent of resection, IDH mutation status, and WHO grade—for OS prediction was performed. All the features, except postoperative treatment, were significantly associated with OS, and were subsequently included for multivariable Cox regression analyses to create prognostic models: 1) clinical model–age, sex, and KPS; 2) clinicopathologic model–age, sex, KPS, extent of resection, IDH mutation status, and WHO grade; and 3) combined clinical and radiomics model. To assess and compare model performance, the integrated area under the curve (iAUC) from a time-dependent receiver operating characteristic (ROC) curve[31] and the C-index of each model were calculated. Differences in those metrics between models were tested based on a 95% confidence interval (CI) from the bootstrap with 1000 resampling. The difference was considered statistically significant if the 95% CI of the difference did not contain a zero value.

Construction of the radiomics nomogram

Based on the multivariable Cox regression, a radiomics nomogram integrating the RRS and clinical features was constructed to predict the OS.[32] The discriminative ability of the nomogram was quantitatively measured using the C-index. Calibration curves were plotted using the observed probabilities and the nomogram-estimated probabilities in both training and test sets.[33]

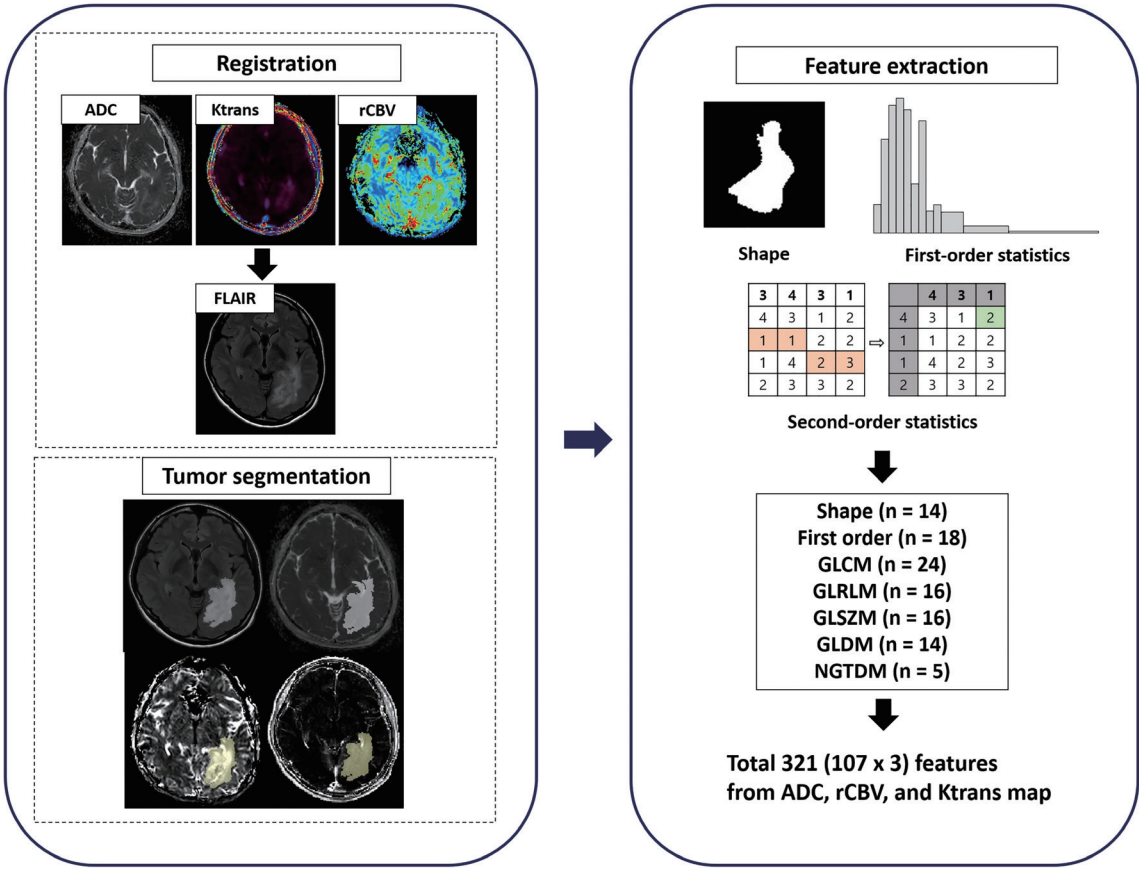

Fig. 2. Radiomics pipeline. ADC, apparent diffusion coefficient; rCBV, relative cerebral blood volume; FLAIR, fluid-attenuated inversion recovery; GLCM, gray level co-occurrence matrix; GLRLM, gray level run-length matrix; GLSZM, gray level size zone matrix; GLDM, gray level dependence matrix; NGTDM, neighboring gray tone difference matrix.

Statistical analysis

Statistical analysis was performed using the R software (version 3.5.1; R Foundation for Statistical Computing, Vienna, Austria). For comparisons between the training and test sets, student's t test, and either chi-square test or Fisher's exact test were performed for continuous and categorical variables, respectively. The LASSO analysis was based on the glmnet package. The optimal cut-off values of the RRSs were defined by the log-rank test using the Contal and O'Quigley's method, which was performed using the "cutp" function of "survMisc" in R.[34] Patients in the training and test sets were then classified into low-risk and high-risk groups according to a fixed cut-off value derived from the training set, and the Kaplan-Meier curves from both groups in the training and test sets were compared. The proportional hazards assumption for the Cox models was tested and satisfied. The nomogram and calibration curves were established using the rms package. A p value<0.05 was considered statistically significant.

RESULTS

The characteristics of the 129 enrolled patients are summarized in Table 1. In the training and test sets, the median OS was 961 days (interquartile range, 737–1543 days) and 2251 days (interquartile range, 1593–2482 days), respectively. There were no significant differences in clinicopathologic characteristics between the training and test sets.

Radiomics risk score construction

In the training set, the C-indices of three different radiomics models—1) single DWI radiomics, 2) single PWI radiomics, and 3) combined DWI and PWI radiomics—for OS prediction were 0.75 (95% CI 0.64–0.86), 0.753 (95% CI, 0.65–0.85), and 0.81 (95% CI, 0.71–0.89), respectively. Since the combined DWI and PWI radiomics performed better than other single layer radiomics, it was used for further analysis. An RRS derived from 14 selected radiomic features (4 from ADC, 5 from DSC, and 5 from DCE) constituted a combined DWI and PWI radiomics. Detailed descriptions of selected features are presented in Supplementary Table 1 (only online).

The optimal RRS cut-off value of 1.68 was derived from the training set. This cut-off stratified both the training and test sets into low-risk and high-risk groups with statistically different OS (p<0.001, both) (Fig. 3). The clinical and pathologic details of low- and high-risk groups are presented in Supplemen-

https://doi.org/10.3349/ymj.2023.0323

Table 1. Patient Characteristics in Both Training and Test Sets (n=129)

Clinical characteristics	Training set (n=90)	Test set (n=39)	*p* value
Age (yr)	46.3±13.6	45.8±12.0	0.845
Sex (male:female)	46:44	20:19	>0.999
KPS	90.0±11.2	90.0±13.9	0.374
Extent of resection			0.056
Total	32 (35.6)	22 (56.4)	
Subtotal or partial	43 (47.8)	16 (41.0)	
Biopsy	15 (16.7)	1 (2.6)	
WHO grade			0.110
Grade 2	33 (26.7)	21 (53.8)	
Grade 3	57 (63.3)	18 (46.2)	
IDH mutation status			0.190
IDH-mutant	68 (73.9)	19 (51.4)	
IDH-wild type	24 (26.1)	18 (48.6)	
Interval between MRI date and surgery	5 (2–12)	19 (7–20)	0.002
Postoperative treatment			0.001
None	1 (1.1)	4 (10.3)	
Radiation	63 (70.0)	27 (69.2)	
Chemotherapy	0 (0.0)	3 (7.7)	
Radiation+Chemotherapy	26 (28.9)	5 (12.8)	
Overall survival, day	961 (737–1543)	2251 (1593–2482)	0.200
No. of deaths observed	26 (28.9)	13 (33.3)	0.770

KPS, Karnofsky Performance Status; WHO, World Health Organization; IDH, isocitrate dehydrogenase.
Data are presented as mean±standard deviation, n (%), or median (Interquartile range).

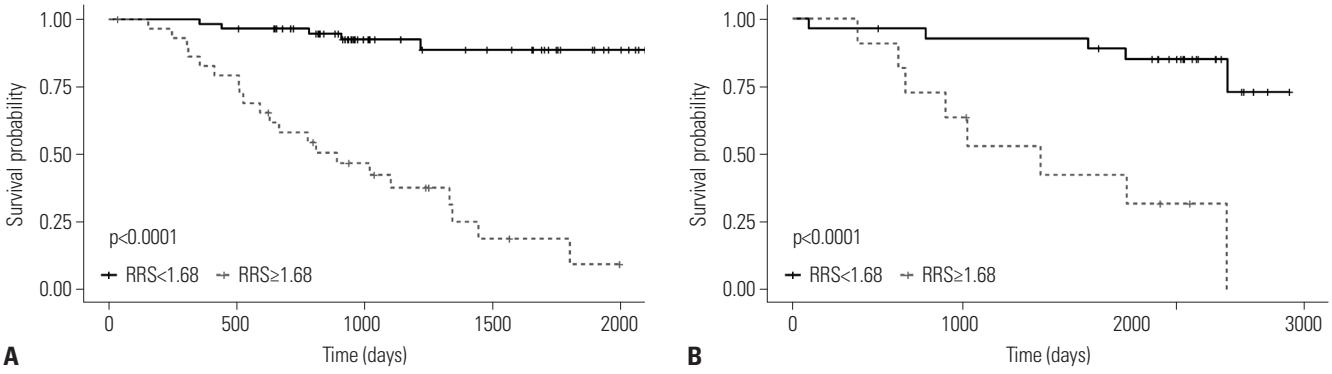

Fig. 3. Kaplan–Meier curves of low-risk and high-risk groups stratified based on the optimal cut-off value in (A) training and (B) test sets. The optimal cut-off value of the radiomics risk score (RRS) was used to stratify patients into two groups with significantly different overall survival in both training and test sets.

tary Table 2 (only online).

Model development and performance evaluation

Multivariate Cox regression analysis created three models (clinical model, clinicopathologic model, and a combined clinical and radiomics model); the hazard ratio (HR) of each variable in the training set is presented in Table 2. Older age and lower KPS were significantly associated with worse prognosis, as observed in all three models. In the clinicopathologic model, IDH mutation status was the most powerful prognostic factor with a HR of 0.14. In the combined clinical and radiomics model, RRS was significantly associated with OS, with a HR of 6.52.

The C-indices of the three different models are presented in Table 3. In the training set, adding DWI and PWI to the clinical model significantly increased the performance from 0.73 (95% CI, 0.65–0.85) to 0.83 (95% CI, 0.75–0.92) (p=0.026). In the test set, adding DWI and PWI to a clinical model also significantly increased the performance from 0.75 (0.64–0.91) to 0.87 (0.80–0.98) (p=0.041). The comparison between the C-index of the combined clinical and radiomics and the clinicopathologic model, which included well-known powerful prognostic factors (i.e., WHO grade and IDH mutation status), showed no significant differences either in the training set or test set.

Time-dependent ROC curves from the clinical and the

Table 2. Three Models Created from Multivariate Cox Regression Analysis in the Training Set

Variables	Clinical model		Clinicopathologic model		Clinical+DWI and PWI radiomics	
	HR (95% CI)	*p* value	HR (95% CI)	*p* value	HR (95% CI)	*p* value
Age	1.04 (1.01–1.07)	0.004	1.03 (1.00–1.06)	0.040	1.04 (1.00–1.07)	0.040
Sex	1.27 (0.58–2.77)	0.550	1.06 (0.47–2.39)	0.900	1.05 (0.46–2.37)	0.910
KPS	0.94 (0.91–0.98)	0.001	0.95 (0.91–0.98)	0.005	0.96 (0.93–0.99)	0.020
Extent of resection	-	-	2.29 (0.63–8.29)	0.210	-	-
WHO grade	-	-	1.94 (0.66–5.70)	0.230	-	-
IDH mutation status	-	-	0.14 (0.05–0.39)	<0.001	-	-
RRS	-	-	-	-	6.52 (2.89–14.71)	<0.001
C-index	0.73 (0.65–0.85)		0.86 (0.80–0.94)		0.83 (0.75–0.92)	

DWI, diffusion-weighted image; PWI, perfusion-weighted image; HR, hazard ratio; CI, confidence interval; KPS, Karnofsky Performance Status; WHO, World Health Organization; IDH, isocitrate dehydrogenase; RRS, radiomics risk score.

Table 3. C-Indices of the Various Models for Overall Survival Prediction in Training and Test Sets

	Training set			Test set		
	C-index	Difference	*p* value	C-index	Difference	*p* value
Clinical+DWI and PWI radiomics	0.83 (0.75–0.92)	Reference	Reference	0.87 (0.80–0.98)	Reference	Reference
Clinical model	0.73 (0.65–0.85)	0.10 (0.02–0.20)	0.026	0.75 (0.64–0.91)	0.12 (0.01–0.25)	0.041
Clinicopathologic model	0.86 (0.80–0.94)	-0.03 (-0.08–0.05)	0.483	0.86 (0.87–0.99)	0.01 (-0.06–0.12)	0.869

DWI, diffusion-weighted image; PWI, perfusion-weighted image.

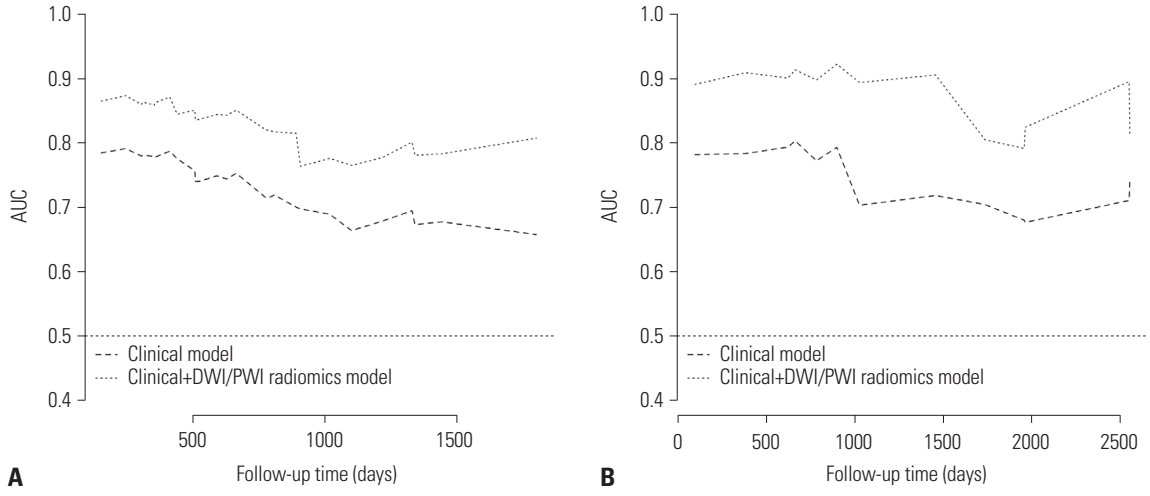

Fig. 4. Time-dependent receiver operating characteristic curves from a clinical model and a combined clinical and radiomics model in (A) training and (B) test sets. AUC, area under the curve; DWI, diffusion-weighted image; PWI, perfusion-weighted image.

combined clinical and radiomics model are shown in Fig. 4. In the training set, the iAUC was significantly higher in the combined model than in the clinical model [0.82 (95% CI, 0.78–0.82) vs. 0.72 (95% CI, 0.68–0.72)]. On bootstrap testing, the increase in iAUC [0.10 (95% CI, 0.07–0.12)] was statistically significant. Similarly, in the test set, when radiomics was added to the clinical model, the iAUC significantly increased from 0.76 (95% CI, 0.64–0.87) to 0.88 (95% CI, 0.80–0.96), with the increase in iAUC [0.12 (95% CI, 0.03–0.24)] being statistically significant.

Radiomics nomogram construction and validation

A radiomics nomogram incorporating the RRS and clinical features was constructed based on multivariate logistic regression (Fig. 5). The corresponding calibration curves demonstrated satisfactory consistency between the nomogram-predicted survival and the actual observed survival in both the training [C-index, 0.83 (95% CI, 0.75–0.92)] and test sets [C-index, 0.87 (95% CI, 0.80–0.98)].

DISCUSSION

In this study, radiomics derived from advanced MRI, such as DWI and PWI, was used to predict survival in patients with lower-grade gliomas. We observed that radiomics derived from

https://doi.org/10.3349/ymj.2023.0323

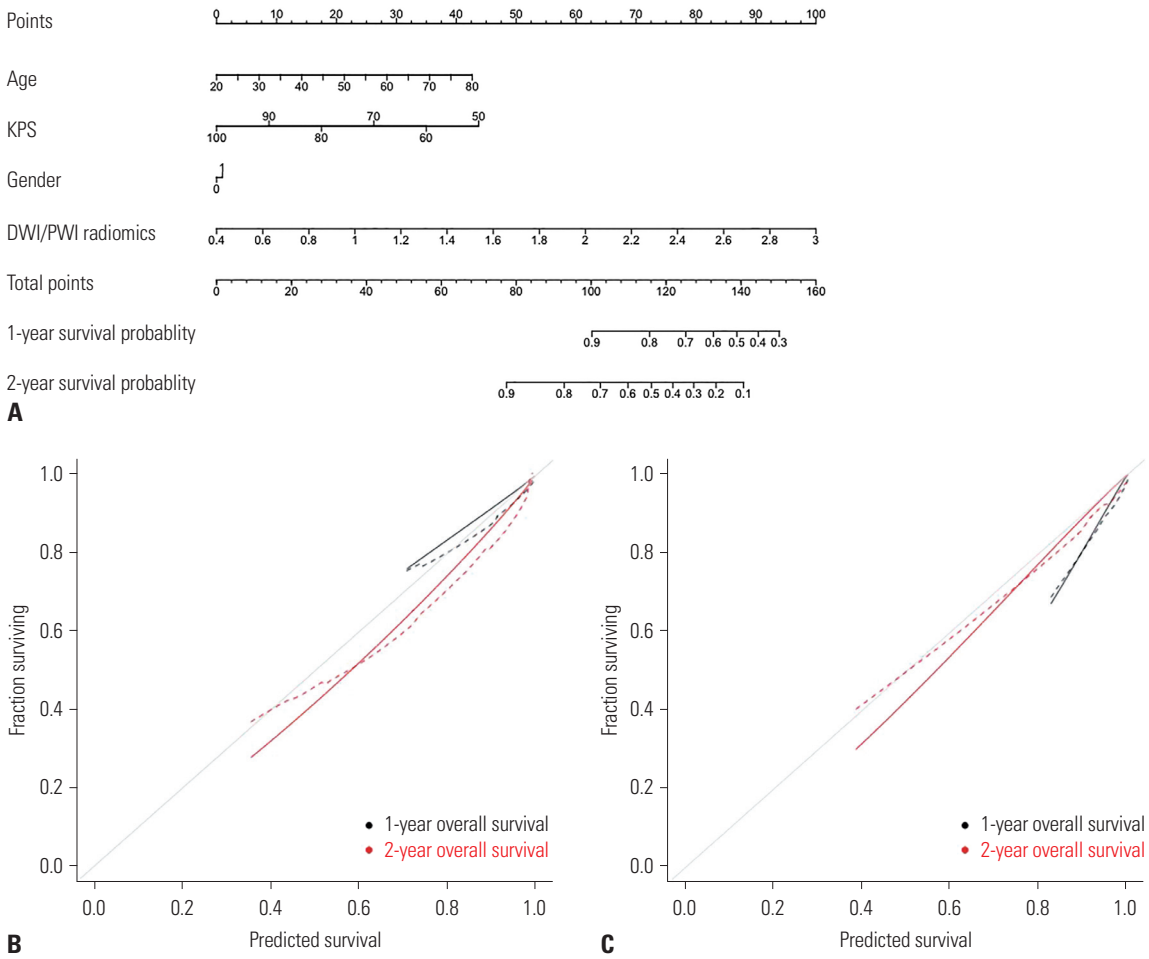

Fig. 5. Nomogram derived from a combined clinical and radiomics model for the prediction of overall survival (A). Calibration curves of the nomogram in the training (B) and test cohorts (C) demonstrated good consistency between the nomogram-estimated survival and actual overall survival. Dotted line represents the original calibration curve, and solid line represents the bias-corrected curve from 100 times of bootstrapping. KPS, Karnofsky Performance Status; DWI, diffusion-weighted image; PWI, perfusion-weighted image.

both DWI and PWI, rather than single layer radiomics, performed better for OS prediction. The optimal RRS cut-off derived from the training set divided the test set into two groups with significantly different survival outcomes, demonstrating the prognostic value of RRS. Furthermore, adding DWI and PWI radiomics to clinical features significantly increased the model performance for OS prediction, as validated in the test set. Calibration curves proved the prognostic accuracy of a nomogram constructed from clinical features and radiomics. Therefore, our study suggests that DWI and PWI radiomics may allow non-invasive risk stratification of patients with lower-grade gliomas and can be used as a potential imaging biomarker.

Little has been studied regarding the prognostic value of advanced MRI radiomics, from either DWI or PWI. Previous studies used advanced MRI radiomics to predict tumor grade and specific genetic mutation status in lower-grade gliomas. The radiomics derived from an ADC map, not FLAIR, provided the highest prediction accuracy for determining the IDH mutation status.[19] Furthermore, most of the top contributing features for the prediction of tumor grades were derived from the ADC map.[18] Multiparametric MRI radiomics, including conventional MRI, ADC, and CBV, also outperformed conventional MRI radiomics in tumor grading.[18] Hence, we focused on the added prognostic role of advanced MRI radiomics, rather than conventional MRI radiomics, over clinical features in patients with lower-grade gliomas. We observed that the RRS from advanced MRI radiomics was one of the independent risk factors for survival prediction. The combined clinical and radiomics model achieved superior performance for OS prediction compared to the clinical model, with iAUC being 0.883 in the test set. Moreover, the performance of the combined model was comparable to that of the clinicopathologic model. It is noteworthy that the model which consisted of only preoperatively available information–age, KPS, gender, and radiomic features–can accurately predict the patient's prognosis to a similar extent compared to the model with pathologic information. The clinicopathologic model included the pathologic information (i.e., the extent of resection, IDH mutation status) and the WHO grade, all of which are well-es-

tablished prognostic factors, which makes its prognostic performance high. Indeed, the clinicopathologic model can accurately predict the prognosis with a C-index of 0.86 in the test set. However, the clinicopathologic model is not feasible in the preoperative setting, as the pathologic information can only be obtained after surgery. As we observed that the combined model with clinical and radiomic features yielded similar prognostic performance compared to the clinicopathologic model (C-index 0.87 vs. 0.86 in the test set, p=0.869) in our study, the combined model can be suggested as a feasible as well as powerful alternative that can be obtained preoperatively.

Numerous studies investigated the prognostic role of perfusion MRI in patients with gliomas, mostly focusing on patients with glioblastomas. The rCBV and Ktrans, obtained from DSC and DCE MRI, respectively, were frequently reported to be significantly negatively correlated with survival, thereby having potential as imaging biomarkers for risk stratification.[35-37] Recently, radiomics has been applied to the rCBV or Ktrans map, showing that perfusion MRI radiomics provided useful information for predicting survival,[38] improved prognostication over clinical features,[39] had significant association with recurrence or progression, and enabled prediction of recurrence pattern[40] in patients with glioblastomas. Even perfusion MRI radiomics derived from non-enhancing T2 hyperintense lesions of glioblastomas can also predict the prognosis and had a significant association with progression-free survival or OS.[41] However, little is known about the prognostic role of perfusion MRI radiomics in lower-grade gliomas. In our study, a single layer perfusion MRI radiomics alone, derived from both rCBV and Ktrans map, could accurately predict the OS with a C-index of 0.753 in the training set. Furthermore, among 14 selected features which constituted a combined DWI and PWI radiomics, 10 were from either rCBV or Ktrans map. Therefore, we believe that PWI radiomics play a significant role in OS prediction not only in patients with glioblastoma but also in those with lower-grade gliomas. Finally, a combined DWI and PWI radiomics model achieved high accuracy for OS prediction when added to clinical features, which proved the added prognostic value of PWI radiomics in patients with lower-grade gliomas.

We then constructed a nomogram from the combined clinical and radiomics model for OS prediction, including age, gender, KPS, and radiomics derived from both DWI and PWI. A previous study using an independently validated nomogram in lower-grade gliomas concluded that grade 2 tumor, younger age at diagnosis, having a high KPS, and the IDH mutant, 1p19q-codeleted molecular subtype, increased the probability of survival.[42] This nomogram included clinically relevant pathologic features, such as the WHO grade and molecular subtype. In our study, we only included features that were available in the preoperative setting, so that the nomogram can calculate individualized survival probabilities before surgery. In addition, DWI and PWI radiomics from preoperative MRI were added. Our clinical and radiomics model was proven to be an effective tool for providing individualized survival probabilities with a C-index of 0.833 in the test set and good calibration.

The top contributing feature for the OS prediction was the skewness from ADC, a first-order feature. Skewness, a histogram parameter, denotes an asymmetric distribution. As lower ADC values and their heterogeneity reflect increased tumor cellularity and heterogeneity,[43] ADC skewness may have a significant association with survival. Among the 14 selected features, half were texture features, which quantify the image pattern based on the spatial relationship or co-occurrence of pixel values[44] and provide information on intratumoral heterogeneity.[12] In gliomas, intratumoral heterogeneity has been reportedly associated with aggressive tumor behavior and drug resistance;[45] therefore, texture features may play a key role in predicting the prognosis.

The present study had several limitations. First, this was a retrospective study with a relatively small sample size, as only patients with lower-grade glioma with both preoperative DSC and DCE MRI were included. Identification of an external validation set with patients having those same characteristics was not feasible; therefore, we performed temporal validation. Further studies using a larger cohort are required to validate our results. Second, important prognostic molecular markers, such as epidermal growth factor receptor amplification or telomerase reverse transcriptase gene promoter mutation, were not included in our analysis due to the lack of information in a considerable number of patients. Future studies may help validate the prognostic role of advanced MRI radiomics in consideration of those important molecular markers.

In conclusion, diffusion- and perfusion-weighted MRI radiomics enables non-invasive risk stratification and can improve survival prediction when added to the clinical features in patients with lower-grade gliomas.

ACKNOWLEDGEMENTS

This research received funding from the Basic Science Research Program through the National Research Foundation of Korea (NRF) funded by the Ministry of Science, Information and Communication Technologies & Future Planning (2020R1A2C1003886), and a grant from the Korea Health Technology R&D Project through the Korea Health Industry Development Institute funded by the Ministry of Health & Welfare, Republic of Korea (HI21C1161). This work was supported by the Korea Medical Device Development Fund grant funded by the Korean government (the Ministry of Science and ICT, the Ministry of Trade, Industry and Energy, the Ministry of Health & Welfare, the Ministry of Food and Drug Safety) (Project Number: RS-2023-00224382).

AUTHOR CONTRIBUTIONS

Conceptualization: Sung Soo Ahn. Data curation: Chae Jung Park and

https://doi.org/10.3349/ymj.2023.0323

Yae Won Park. Formal analysis: Kyunghwa Han and Sooyon Kim. Funding acquisition: Sung Soo Ahn. Investigation: Chae Jung Park and Dain Kim. Methodology: Kyunghwa Han, Sooyon Kim, and Dain Kim. Project administration: Seung-Koo Lee and Sung Soo Ahn. Resources: Se Hoon Kim and Jong Hee Chang. Software: Chae Jung Park and Dain Kim. Supervision: Se Hoon Kim, Jong Hee Chang, and Seung-Koo Lee. Validation: Kyunghwa Han and Sooyon Kim. Visualization: Yae Won Park. Writing—original draft: Chae Jung Park and Yae Won Park. Writing—review & editing: Sung Soo Ahn, Jong Hee Chang, and Seung-Koo Lee. Approval of final manuscript: all authors.

ORCID iDs

Chae Jung Park https://orcid.org/0000-0002-5567-8658
Sooyon Kim https://orcid.org/0000-0003-1607-6475
Kyunghwa Han https://orcid.org/0000-0002-5687-7237
Sung Soo Ahn https://orcid.org/0000-0002-0503-5558
Dain Kim https://orcid.org/0000-0003-3425-0182
Yae Won Park https://orcid.org/0000-0001-8907-5401
Jong Hee Chang https://orcid.org/0000-0003-1509-9800
Se Hoon Kim https://orcid.org/0000-0001-7516-7372
Seung-Koo Lee https://orcid.org/0000-0001-5646-4072

REFERENCES

1. Brat DJ, Verhaak RG, Aldape KD, Yung WK, Salama SR, Cooper LA, et al. Comprehensive, integrative genomic analysis of diffuse lower-grade gliomas. N Engl J Med 2015;372:2481-98.
2. Yan H, Parsons DW, Jin G, McLendon R, Rasheed BA, Yuan W, et al. IDH1 and IDH2 mutations in gliomas. N Engl J Med 2009;360:765-73.
3. Louis DN, Perry A, Wesseling P, Brat DJ, Cree IA, Figarella-Branger D, et al. The 2021 WHO classification of tumors of the central nervous system: a summary. Neuro Oncol 2021;23:1231-51.
4. Aibaidula A, Chan AK, Shi Z, Li Y, Zhang R, Yang R, et al. Adult IDH wild-type lower-grade gliomas should be further stratified. Neuro Oncol 2017;19:1327-37.
5. Brat DJ, Aldape K, Colman H, Holland EC, Louis DN, Jenkins RB, et al. cIMPACT-NOW update 3: recommended diagnostic criteria for "diffuse astrocytic glioma, IDH-wildtype, with molecular features of glioblastoma, WHO grade IV". Acta Neuropathol 2018;136:805-10.
6. Oberheim Bush NA, Chang S. Treatment strategies for low-grade glioma in adults. J Oncol Pract 2016;12:1235-41.
7. Douw L, Klein M, Fagel SS, van den Heuvel J, Taphoorn MJ, Aaronson NK, et al. Cognitive and radiological effects of radiotherapy in patients with low-grade glioma: long-term follow-up. Lancet Neurol 2009;8:810-8.
8. van Dijken BRJ, van Laar PJ, Smits M, Dankbaar JW, Enting RH, van der Hoorn A. Perfusion MRI in treatment evaluation of glioblastomas: clinical relevance of current and future techniques. J Magn Reson Imaging 2019;49:11-22.
9. Choi YS, Ahn SS, Lee HJ, Chang JH, Kang SG, Kim EH, et al. The initial area under the curve derived from dynamic contrast-enhanced MRI improves prognosis prediction in glioblastoma with unmethylated MGMT promoter. AJNR Am J Neuroradiol 2017;38:1528-35.
10. Villanueva-Meyer JE, Wood MD, Choi BS, Mabray MC, Butowski NA, Tihan T, et al. MRI features and IDH mutational status of grade II diffuse gliomas: impact on diagnosis and prognosis. AJR Am J Roentgenol 2018;210:621-8.
11. Leu K, Ott GA, Lai A, Nghiemphu PL, Pope WB, Yong WH, et al. Perfusion and diffusion MRI signatures in histologic and genetic subtypes of WHO grade II-III diffuse gliomas. J Neurooncol 2017;134:177-88.
12. Gillies RJ, Kinahan PE, Hricak H. Radiomics: images are more than pictures, they are data. Radiology 2016;278:563-77.
13. Aerts HJ, Velazquez ER, Leijenaar RT, Parmar C, Grossmann P, Carvalho S, et al. Decoding tumour phenotype by noninvasive imaging using a quantitative radiomics approach. Nat Commun 2014;5:4006.
14. Park CJ, Han K, Kim H, Ahn SS, Choi D, Park YW, et al. MRI features may predict molecular features of glioblastoma in isocitrate dehydrogenase wild-type lower-grade gliomas. AJNR Am J Neuroradiol 2021;42:448-56.
15. Park CJ, Han K, Kim H, Ahn SS, Choi YS, Park YW, et al. Radiomics risk score may be a potential imaging biomarker for predicting survival in isocitrate dehydrogenase wild-type lower-grade gliomas. Eur Radiol 2020;30:6464-74.
16. Choi YS, Ahn SS, Chang JH, Kang SG, Kim EH, Kim SH, et al. Machine learning and radiomic phenotyping of lower grade gliomas: improving survival prediction. Eur Radiol 2020;30:3834-42.
17. Wang J, Zheng X, Zhang J, Xue H, Wang L, Jing R, et al. An MRI-based radiomics signature as a pretreatment noninvasive predictor of overall survival and chemotherapeutic benefits in lower-grade gliomas. Eur Radiol 2021;31:1785-94.
18. Kim M, Jung SY, Park JE, Jo Y, Park SY, Nam SJ, et al. Diffusion- and perfusion-weighted MRI radiomics model may predict isocitrate dehydrogenase (IDH) mutation and tumor aggressiveness in diffuse lower grade glioma. Eur Radiol 2020;30:2142-51.
19. Ren Y, Zhang X, Rui W, Pang H, Qiu T, Wang J, et al. Noninvasive prediction of IDH1 mutation and ATRX expression loss in low-grade gliomas using multiparametric MR radiomic features. J Magn Reson Imaging 2019;49:808-17.
20. Kim KJ, Park M, Joo B, Ahn SJ, Suh SH. Dynamic contrast-enhanced MRI and its applications in various central nervous system diseases. Investig Magn Reson Imaging 2022;26:256-64.
21. Choi HS, Kim AH, Ahn SS, Shin NY, Kim J, Lee SK. Glioma grading capability: comparisons among parameters from dynamic contrast-enhanced MRI and ADC value on DWI. Korean J Radiol 2013;14:487-92.
22. Jung SC, Yeom JA, Kim JH, Ryoo I, Kim SC, Shin H, et al. Glioma: application of histogram analysis of pharmacokinetic parameters from T1-weighted dynamic contrast-enhanced MR imaging to tumor grading. AJNR Am J Neuroradiol 2014;35:1103-10.
23. Ahn SH, Ahn SS, Park YW, Park CJ, Lee SK. Association of dynamic susceptibility contrast- and dynamic contrast-enhanced magnetic resonance imaging parameters with molecular marker status in lower-grade gliomas: a retrospective study. Neuroradiol J 2023;36:49-58.
24. Morabito R, Alafaci C, Pergolizzi S, Pontoriero A, Iati' G, Bonanno L, et al. DCE and DSC perfusion MRI diagnostic accuracy in the follow-up of primary and metastatic intra-axial brain tumors treated by radiosurgery with cyberknife. Radiat Oncol 2019;14:65.
25. Elshafeey N, Kotrotsou A, Hassan A, Elshafei N, Hassan I, Ahmed S, et al. Multicenter study demonstrates radiomic features derived from magnetic resonance perfusion images identify pseudoprogression in glioblastoma. Nat Commun 2019;10:3170.
26. Shiroishi MS, Castellazzi G, Boxerman JL, D'Amore F, Essig M, Nguyen TB, et al. Principles of T2*-weighted dynamic susceptibility contrast MRI technique in brain tumor imaging. J Magn Reson Imaging 2015;41:296-313.
27. Fedorov A, Beichel R, Kalpathy-Cramer J, Finet J, Fillion-Robin JC, Pujol S, et al. 3D Slicer as an image computing platform for the Quantitative Imaging Network. Magn Reson Imaging 2012;30:1323-41.

28. van Griethuysen JJM, Fedorov A, Parmar C, Hosny A, Aucoin N, Narayan V, et al. Computational radiomics system to decode the radiographic phenotype. Cancer Res 2017;77:e104-7.
29. Zwanenburg A, Vallières M, Abdalah MA, Aerts HJWL, Andrearczyk V, Apte A, et al. The image biomarker standardization initiative: standardized quantitative radiomics for high-throughput image-based phenotyping. Radiology 2020;295:328-38.
30. Friedman J, Hastie T, Tibshirani R. Regularization paths for generalized linear models via coordinate descent. J Stat Softw 2010;33:1-22.
31. Heagerty PJ, Zheng Y. Survival model predictive accuracy and ROC curves. Biometrics 2005;61:92-105.
32. Iasonos A, Schrag D, Raj GV, Panageas KS. How to build and interpret a nomogram for cancer prognosis. J Clin Oncol 2008;26:1364-70.
33. Balachandran VP, Gonen M, Smith JJ, DeMatteo RP. Nomograms in oncology: more than meets the eye. Lancet Oncol 2015;16:e173-80.
34. Contal C, O'Quigley J. An application of changepoint methods in studying the effect of age on survival in breast cancer. Comput Stat Data Anal 1999;30:253-70.
35. Schmainda KM, Zhang Z, Prah M, Snyder BS, Gilbert MR, Sorensen AG, et al. Dynamic susceptibility contrast MRI measures of relative cerebral blood volume as a prognostic marker for overall survival in recurrent glioblastoma: results from the ACRIN 6677/RTOG 0625 multicenter trial. Neuro Oncol 2015;17:1148-56.
36. Larsson C, Groote I, Vardal J, Kleppestø M, Odland A, Brandal P, et al. Prediction of survival and progression in glioblastoma patients using temporal perfusion changes during radiochemotherapy. Magn Reson Imaging 2020;68:106-12.
37. Bonekamp D, Deike K, Wiestler B, Wick W, Bendszus M, Radbruch A, et al. Association of overall survival in patients with newly diagnosed glioblastoma with contrast-enhanced perfusion MRI: comparison of intraindividually matched T1- and T2*-based bolus techniques. J Magn Reson Imaging 2015;42:87-96.
38. Lee J, Jain R, Khalil K, Griffith B, Bosca R, Rao G, et al. Texture feature ratios from relative CBV maps of perfusion MRI are associated with patient survival in glioblastoma. AJNR Am J Neuroradiol 2016;37:37-43.
39. Park JE, Kim HS, Jo Y, Yoo RE, Choi SH, Nam SJ, et al. Radiomics prognostication model in glioblastoma using diffusion- and perfusion-weighted MRI. Sci Rep 2020;10:4250.
40. Shim KY, Chung SW, Jeong JH, Hwang I, Park CK, Kim TM, et al. Radiomics-based neural network predicts recurrence patterns in glioblastoma using dynamic susceptibility contrast-enhanced MRI. Sci Rep 2021;11:9974.
41. Pak E, Choi KS, Choi SH, Park CK, Kim TM, Park SH, et al. Prediction of prognosis in glioblastoma using radiomics features of dynamic contrast-enhanced MRI. Korean J Radiol 2021;22:1514-24.
42. Gittleman H, Sloan AE, Barnholtz-Sloan JS. An independently validated survival nomogram for lower-grade glioma. Neuro Oncol 2020;22:665-74.
43. Eidel O, Neumann JO, Burth S, Kieslich PJ, Jungk C, Sahm F, et al. Automatic analysis of cellularity in glioblastoma and correlation with ADC using trajectory analysis and automatic nuclei counting. PLoS One 2016;11:e0160250.
44. Soni N, Priya S, Bathla G. Texture analysis in cerebral gliomas: a review of the literature. AJNR Am J Neuroradiol 2019;40:928-34.
45. Meyer M, Reimand J, Lan X, Head R, Zhu X, Kushida M, et al. Single cell-derived clonal analysis of human glioblastoma links functional and genomic heterogeneity. Proc Natl Acad Sci U S A 2015;112:851-6.

https://doi.org/10.3349/ymj.2023.0323